J. Phys. Soc. Jpn. Downloaded from journals.jps.jp by University of California San Diego on 03/05/17

Journal of the Physical Society of Japan
Vol. 65, No. 9, September, 1996, pp. 2811-2823

# A Detailed Study of Power Spectral Density for Rossler System

Norio OHTOMO, Ayako SUMI[1], Yukio TANAKA[2],
Kazuo TOKIWANO and Saburou TERACHI[3]

*Faculty of Engineering, Hokkaido University, Sapporo 060*
[1]*Hokkaido University School of Medicine, Sapporo 060*
[2]*Suwa Trust Co., Ltd., Ohmori, Tokyo 143*
[3]*Hokkaido Institute of Technology, Sapporo 006*

(Received September 28, 1995)

Power spectral densities (PSD's) calculated by the maximum entropy method (MEM) for Rossler system indicated exponential decay with a large number of well-defined spectral lines. The spectral lines were confirmed to indicate a complete bifurcation up to the fifth-order period-doubling. An extremely anomalous behavior was recognized in the region of $c = 4.18$–$4.21$ which is considered to be a transition region. The contribution of the power of the fundamental mode to the total power was overwhelmingly large: it becomes larger than 90%. A prediction of time series including chaotic ones was performed and the satisfactory results obtained. It will be discussed that the fluctuations due to amplitude instability of time series in the periodic solutions generate, resulting in the continuous component of PSD structured through the subharmonic cascade process, and this continuous region is restructured in the inverse cascade process (the socalled broad continuum in the chaotic mixing).

KEYWORDS: Rossler model, nonlinear equation, chaotic time series, power spectral density (PSD), maximum entorpy method (MEM), exponential spectrum, subharmonic bifurcation, inverse cascade, fundamental mode, time series prediction

## §1. Introduction

Many works have been carried out for spectral analysis of chaotic time series in theoretical and experimental points of view and some of the results are summarized in several monographs.[1-3] Researchers have established a conclusion that the power spectra of chaotic time series show power lows in the form $f^{-\beta}$ ($f$: frequency). Especially, in the case of $\beta = 1$ the socalled "$1/f$ noise" has been well-known as an intermittent chaotic phenomena. On the other hand, many experimental and theoretical studies have reported the power spectra of exponential form: $\exp(-\lambda f)$.[4-12] Among them, Frisch and Morf reported in their theoretical work[10] that the very-high-frequency behavior of the power spectrum shows up the overall amplitude decreasing exponentially. And, the exponential decrease of PSD has been widely found out in many experimental works on turbulence.[4,5,9] In addition, it was confirmed in our preceding paper[13] that the behaviors of power spectral densities (PSD's) for nonlinear systems such as Lorenz, Rossler and Duffing models universally exhibit exponential characteristics. Therein, it was concluded that exponential spectra are caused by nonlinear phenomena including chaotic motions. However, we are scarce of systematic works on the spectral analysis of time series generated from nonlinear systems.

In the present study, we attempt to investigate comprehensively, in detail, the time series generated by Rossler system throughout a series of bifurcations as well as chaotic regime.

## §2. Time Series for Rossler Model

### 2.1 *Rossler model and parameters used*

Rossler model is described by

$$\begin{aligned} dX/dt &= -Y - Z \\ dY/dt &= X + aY \\ dZ/dt &= b + XZ - cZ \end{aligned} \tag{1}$$

where $X$, $Y$ and $Z$ are variables, $a$, $b$ and $c$ parameters to be chosen. In the present study, we used $a = b = 0.2$. With respect to the third parameter $c$, nine values (2.6, 3.5, 4.1, 4.18, 4.21, 4.23, 4.30, 4.60 and 5.7) were adopted. The first eight values of parameter $c$ correspond to A–H denoted in Fig. 3 in Crutchfield *et al.*'s paper[3] where the largest Lyapunov characteristic exponents are plotted as a function of parameter $c$. The last three values correspond to the chaotic regime, among them $c = 5.7$ being the growest state of chaos.

### 2.2 *Time series*

We solved numerically the differential eqs. (1) using the fourth order Runge-Kutta algorithm with the time interval $\Delta t = 0.01$ (arbitrary unit) and the initial values $X_0 = Y_0 = Z_0 = 1.0$. The calculations were performed over 36000 steps (the time range 0–360). For the present analysis, we averaged every five steps and the resultant data become 7200 points.

For each parameter value of $c$, the time series $X$ are shown in Fig. 1 (the upper figure in the left side for each parameter), accompanied with some of the results obtained for the corresponding time series. It is easily seen in the figure that the maximum amplitudes of time se-

J. Phys. Soc. Jpn. Downloaded from journals.jps.jp by University of California San Diego on 03/05/17



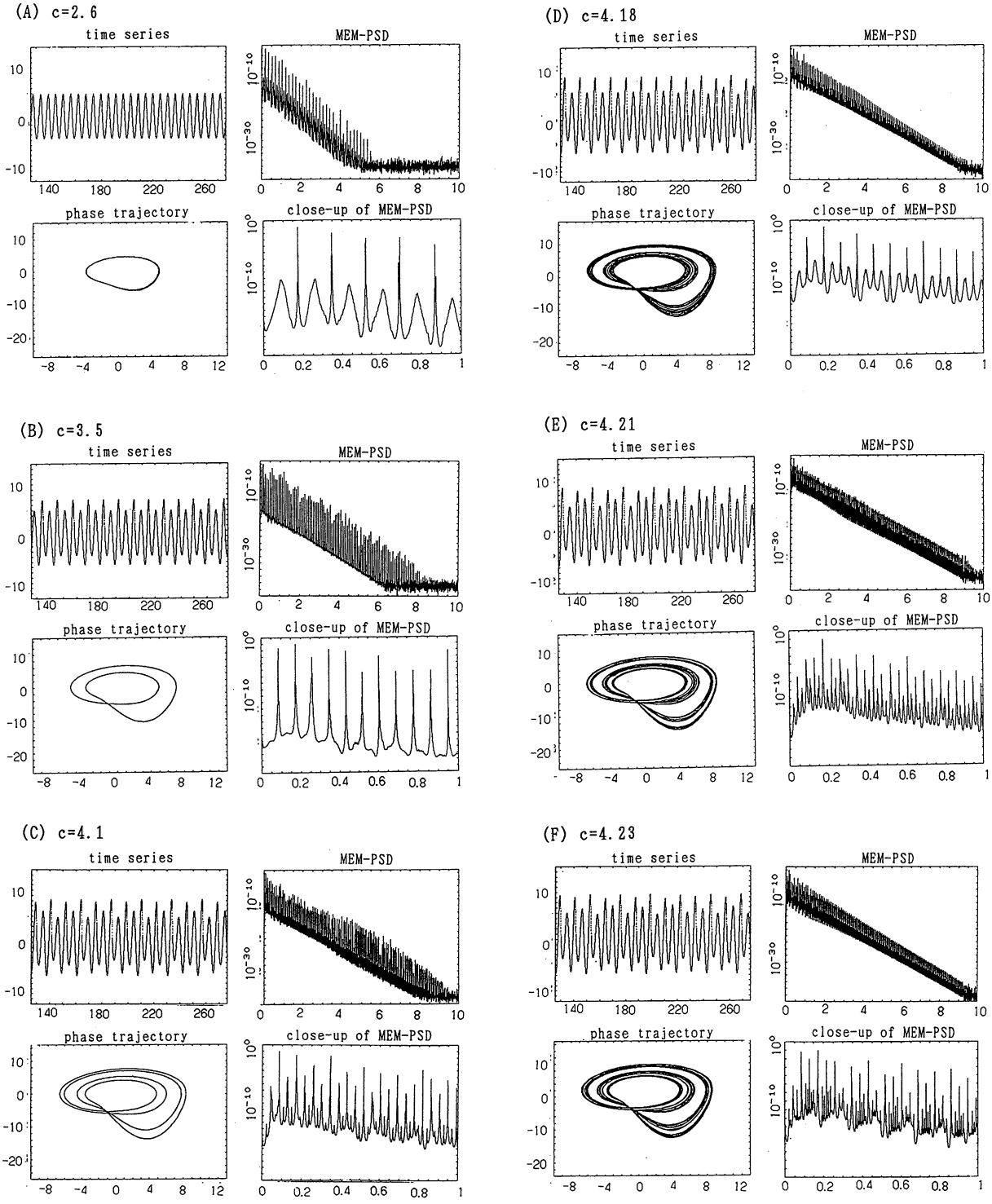


Fig. 1. Original time series, phase trajectory and MEM-PSD for every values of parameter $c$. (A) $c = 2.6$, (B) $c = 3.5$, (C) $c = 4.1$, (D) $c = 4.18$, (E) $c = 4.21$, (F) $c = 4.23$, (G) $c = 4.30$, (H) $c = 4.60$ and (I) $c = 5.7$. For every parameter, the upper figure in the left side: original time series, the lower figure in the left side: its phase trajectory, the upper figure in the right side: MEM-PSD (semi-log scale), and the lower figure in the right side: the close-up of the MEM-PSD.

ries and fluctuations of amplitudes gradually increase as the value of $c$ increases, and that the wave trains largely fluctuate on the approach of $c = 5.7$.

### *2.3 Phase trajectory*

Phase trajectory on the $dX/dt$-$X$ plane was obtained after transients (>1000 points). The phase trajectories are drawn directly below each time series in Fig. 1. These results topologically agree with those by Crutchfield *et al.*, although their trajectories are drawn on the $X$-$Y$ plane. From these trajectories, we can easily conjecture a complete bifurcation sequence for the cases of $c = 2.6$, 3.5 and 4.1. The patterns for the cases of $c = 4.18$–$4.30$ are indistinguishable from each other at a glance.

J. Phys. Soc. Jpn. Downloaded from journals.jps.jp by University of California San Diego on 03/05/17



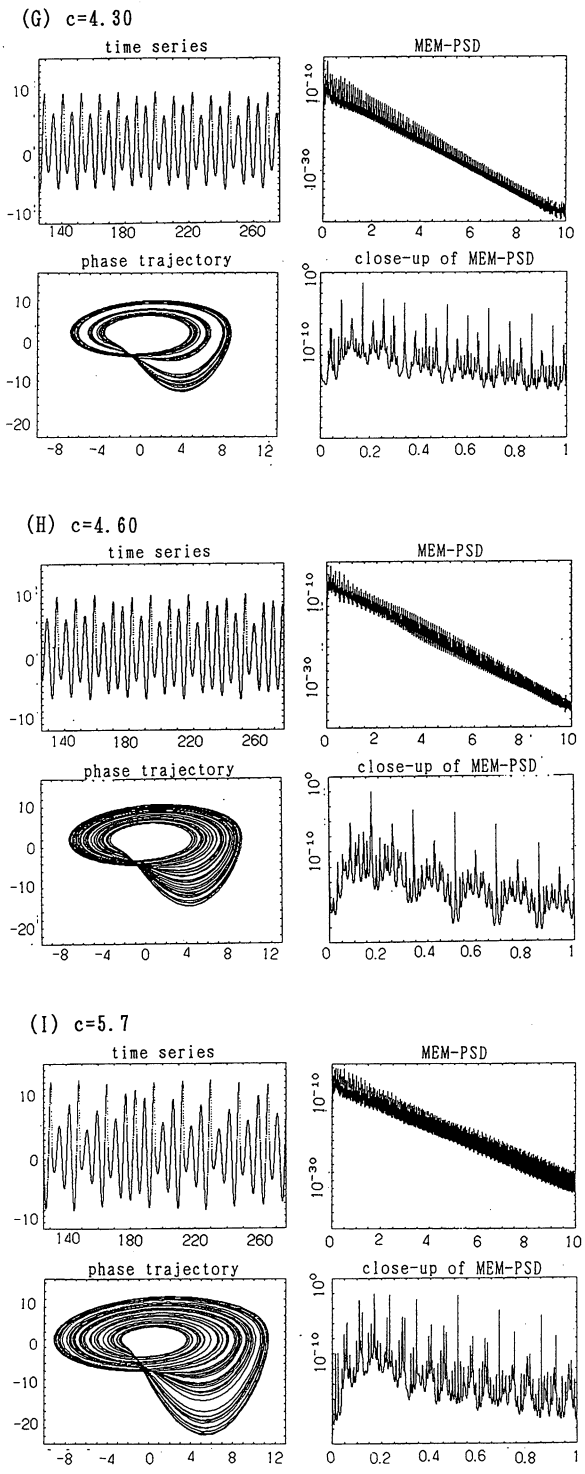


## §3. Power Spectral Densities

The spectral analyses were made for 3000-point data in the time range 125–275, based on the maximum entropy method (MEM). The MEM-PSD's were obtained for each parameter. The formulation of MEM-PSD are described in elsewhere[13-16] (see eq. (4) in ref. 13, for example).

### *3.1 Spectral gradients*

The semi-log plots of MEM-PSD are displayed in Fig. 1 (the upper figure in the right side for each parameter). It

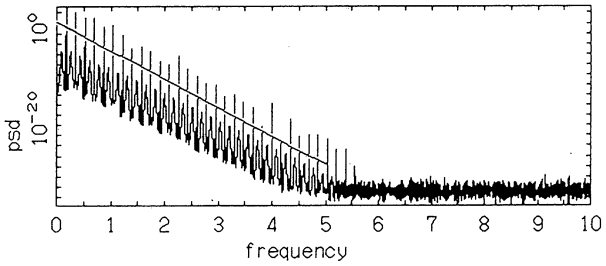


Fig. 2. The close-up of semi-log plots of PSD for $c = 2.6$ shown in Fig. 1.

can be found that the whole spectrum for each parameter universally indicates clearly exponential characteristics until it levels off at a limit determined by the accuracy of the present computation. That is, the overall trend of the PSD can be described as an exponential form

$$P(f) \sim \exp(-\lambda f) \tag{2}$$

where $\lambda$ is a coefficient of exponent. The close-up of semi-log plots of overall PSD for $c = 2.6$ in Fig. 1 is shown in Fig. 2, indicating an exponential decay with numerous discrete spectral lines. The difference between the top of the spectral line and the bottom becomes the order of 10 in logarithm scale. Then, to obtain the magnitude of $\lambda$, we calculated the mean power of PSD from integrating PSD over small frequency interval $\Delta f$, that is, the mean power of PSD is the power in the interval of frequencies $[f, f + \Delta f]$. The line of PSD gradient is calculated as a regression line against the mean powers, and thus obtained is drawn in Fig. 2. We could determine the precise value of $\lambda$ based on this procedure. The values of $\lambda$ obtained for each parameter are listed in Table I and plotted in Fig. 3.

As cleraly seen in Fig. 3, the values of $\lambda$ decrease as the parameter $c$ increases. The decreasing trend separates two regions (solid and dashed lines indicated in Fig. 3). As stated in §3.2.1 and 3.2.2, the solid line corresponds to a subharmonic cascade and the dashed line an inverse cascade. This result is very interesting as suggesting a difference of period-bifurcation from the inverse cascade. The anomalous behavior around $c = 4.18$–$4.23$ bestriding the boundary between periodic and chaotic

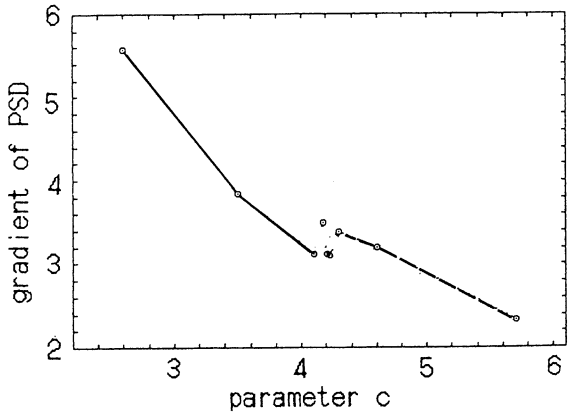


Fig. 3. Gradinets of MEM-PSD against the parameter $c$. Solid line: subharmonic bifurcations, and dashed line: inverse cascade.

J. Phys. Soc. Jpn. Downloaded from journals.jps.jp by University of California San Diego on 03/05/17



Table I. MEM-PSD gradients.

| Parameter $c$ | Gradient $\lambda$ |
|---|---|
| 2.6 | 5.582 |
| 3.5 | 3.843 |
| 4.1 | 3.124 |
| 4.18 | 3.493 |
| 4.21 | 3.124 |
| 4.23 | 3.095 |
| 4.3 | 3.388 |
| 4.6 | 3.202 |
| 5.7 | 2.328 |

domains (Fig. 3 in ref. 3) is considered to correspond to a transition region between two decreasing trends.

### *3.2 Spectral lines*

Figure below each MEM-PSD in Fig. 1 shows the close-up of the range 0–1 of the MEM-PSD. Specifications for each spectral line observed in the frequency range up to the fundamental mode (the frequency of this mode is labelled as $f_1$) are summarized in Table II. From Fig. 1(A)–1(I) and Table II, we can see a cascade of subharmonic bifurcations in the cases of $c = 2.6$, 3.5 and 4.1 and an inverse cascade in the cases of $c = 4.30$. 4.60 and 5.7. The cases of $c = 4.18$, 4.12 and 4.23 are considered to correspond to a transition region. This result slightly differs from that by Crutchfield *et al.* (see Table I in ref. 3).

#### *3.2.1 Subharmonic bifurcations*

Case (A) ($c = 2.6$): the most prominent peak, which corresponds to the fundamental mode, is observed at $f = 0.1737$, and its harmonics are also observed at $f = 0.3476$, 0.5220, 0.6950 and 0.8667.

A broad peak with lower intensity at $f = 0.0903$ is considered to correspond to the first subharmonics (the frequency of this subharmonics is labelled as $f_{1/2}$). The ratio of the power of $f_{1/2}$-mode (0.000003) to that of $f_1$-mode (0.09) becomes $\sim 10^{-5}$, and consequently, the contribution of $f_{1/2}$-subharmonics to the total power becomes 0.0008% and is negligibly small. Thus, in the case of $c = 2.6$, it can be considered that only one fundamental mode occurs substantially.

Case (B) ($c = 3.5$): sharp spectral line at $f = 0.1733$ corresponds to the fundamental mode ($f_1$), and those at $f = 0.3460$, 0.5192, 0.6929 and 0.8660 correspond to its harmonics ($f_2$, $f_3$, $f_4$ and $f_5$, respectively). Like, sharp spectral lines observed at $f = 0.0867$, 0.2595, 0.4331, 0.6066, 0.7795 and 0.9528 correspond to the first subharmonics and its odd harmonics ($f_{1/2}$, $f_{3/2}$, $f_{5/2}$, $f_{7/2}$, $f_{9/2}$ and $f_{11/2}$, respectively). It can be understood that

Table II. Contribution of dominant subharmonics and harmonics. —: negligible small, ∗: unused for LSF.

| Parameter $c$ | MEM-PSD mode | Frequency | Period | Optimum LSF Curve phase | amplitude $A_i$ | Squared amplitude $A_i^2$ | Contribution $A_i^2/Q$ (%) |
|---|---|---|---|---|---|---|---|
| (A) 2.6 | $f_1$ | 0.1737 | 5.757 | 0.999 | 4.3183 | 18.6477 | 98.901 |
| | | | | residual $SD^2$ | | 0.0023 | 0.012 |
| | | | | total power $Q$ | | 18.8551 | 100.001 |
| (B) 3.5 | $f_{1/2}$ | 0.0867 | 11.534 | 10.151 | 0.7780 | 0.6053 | 2.112 |
| | $f_1$ | 0.1733 | 5.770 | 1.460 | 5.1856 | 26.8904 | 93.837 |
| | | | | residual $SD^2$ | | 0.0080 | 0.028 |
| | | | | total power $Q$ | | 28.6567 | 100.000 |
| (C) 4.1 | $f_{1/4}$ | 0.0435 | 23.015 | 5.011 | 0.0722 | 0.0052 | 0.002 |
| | $f_{1/2}$ | 0.0863 | 11.585 | 4.441 | 0.8891 | 0.7905 | 0.317 |
| | $f_{3/4}$ | 0.1285 | 7.727 | 4.214 | 0.4523 | 0.2045 | 0.082 |
| | $f_1$ | 0.1726 | 5.793 | 1.536 | 15.7268 | 247.3322 | 99.135 |
| | | | | residual $SD^2$ | | 0.0055 | 0.002 |
| | | | | total power $Q$ | | 249.4919 | 99.999 |
| (D) 4.18 | $f_{1/4}$ | 0.0436 | 22.941 | 4.750 | 0.0367 | 0.0013 | 0.002 |
| | | 0.0484 | 20.642 | 10.827 | 0.0354 | 0.0013 | 0.002 |
| | $f_{1/2}$ | 0.0866 | 11.544 | 4.858 | 0.6651 | 0.4423 | 0.787 |
| | | 0.0851 | 11.746 | 2.571 | 0.3530 | 0.1246 | 0.222 |
| | $f_{3/4}$ | 0.1276 | 7.839 | 0.972 | 0.1973 | 0.0389 | 0.069 |
| | $f_1$ | 0.1729 | 5.796 | 1.578 | 7.3531 | 54.0686 | 96.228 |
| | | | | residual $SD^2$ | | 0.0030 | 0.053 |
| | | | | total power $Q$ | | 56.1880 | 98.998 |
| (E) 4.21 | $f_{1/8}$ | 0.0238 | 41.997 | ∗ | ∗ | ∗ | ∗ |
| | $f_{1/4}$ | 0.0431 | 23.204 | 8.215 | 0.0484 | 0.0023 | 0.019 |
| | $f_{3/8}$ | 0.0648 | 15.429 | 12.662 | 0.0307 | 0.0009 | 0.005 |
| | $f_{1/2}$ | 0.0866 | 11.554 | 5.122 | 0.8920 | 0.7957 | 3.801 |
| | $f_{5/8}$ | 0.1061 | 9.422 | 6.673 | 0.0748 | 0.0056 | 0.027 |
| | $f_{3/4}$ | 0.1290 | 7.754 | 7.598 | 0.4843 | 0.2345 | 1.120 |
| | $f_{7/8}$ | 0.1517 | 6.593 | 1.764 | 0.0728 | 0.0053 | 0.025 |
| | $f_1$ | 0.1723 | 5.819 | 0.864 | 4.1972 | 17.6164 | 84.156 |
| | | | | residual $SD^2$ | | 0.0115 | 0.055 |
| | | | | total power $Q$ | | 20.9330 | 99.582 |

J. Phys. Soc. Jpn. Downloaded from journals.jps.jp by University of California San Diego on 03/05/17



| Parameter $c$ | MEM-PSD mode | Frequency | Period | Optimum LSF Curve phase | amplitude $A_i$ | Squared amplitude $A_i^2$ | Contribution $A_i^2/Q$ (%) |
|---|---|---|---|---|---|---|---|
| (F) 4.23 | $(f_{1/16})$ | | | | | | |
| | $f_{1/8}$ | 0.0217 | 46.18 | 1.322 | 0.0063 | — | — |
| | $(f_{3/16})$ | | | | | | |
| | $f_{1/4}$ | 0.0416 | 24.06 | 8.401 | 0.0462 | 0.0021 | 0.007 |
| | $f_{5/16}$ | 0.0539 | 18.53 | * | * | * | * |
| | $f_{3/8}$ | 0.0644 | 15.54 | 2.356 | 0.0388 | 0.0015 | 0.003 |
| | $f_{7/16}$ | 0.0745 | 13.42 | * | * | * | * |
| | $f_{1/2}$ | 0.0865 | 11.56 | 5.049 | 1.1048 | 1.2205 | 2.710 |
| | $f_{9/16}$ | 0.1036 | 9.652 | 6.234 | 0.0312 | 0.0009 | 0.002 |
| | $f_{5/8}$ | 0.1094 | 9.138 | 8.116 | 0.0859 | 0.0074 | 0.016 |
| | $f_{11/16}$ | 0.1202 | 8.321 | 2.740 | 0.0517 | 0.0027 | 0.006 |
| | $f_{3/4}$ | 0.1292 | 7.738 | 0.285 | 0.4565 | 0.2084 | 0.463 |
| | $f_{13/16}$ | 0.1392 | 7.183 | 6.581 | 0.0510 | 0.0026 | 0.006 |
| | $f_{7/8}$ | 0.1484 | 6.738 | 0.401 | 0.0642 | 0.0041 | 0.009 |
| | $f_{15/16}$ | 0.1700 | 5.882 | 4.651 | 0.3416 | 0.1167 | 0.259 |
| | $f_1$ | 0.1725 | 5.797 | 1.657 | 6.4332 | 41.3864 | 91.890 |
| | | | | residual $SD^2$ | | 0.0078 | 0.017 |
| | | | | total power $Q$ | | 45.0392 | 99.996 |
| (G) 4.30 | | 0.0408 | 24.515 | 1.726 | 0.0514 | 0.0026 | 0.007 |
| | $f_{1/4}$ | 0.0445 | 22.477 | 1.189 | 0.0563 | 0.0032 | 0.008 |
| | | 0.0562 | 17.793 | * | * | * | * |
| | | 0.0737 | 13.566 | * | * | * | * |
| | $f_{1/2}$ | 0.0860 | 11.628 | 4.669 | 0.9528 | 0.9079 | 2.394 |
| | | 0.0869 | 11.508 | 3.288 | 0.3422 | 0.1171 | 0.309 |
| | | 0.1006 | 9.938 | 7.873 | 0.0467 | 0.0022 | 0.006 |
| | | 0.1122 | 8.915 | 7.699 | 0.0371 | 0.0014 | 0.004 |
| | $f_{3/4}$ | 0.1274 | 7.848 | 4.568 | 0.2924 | 0.0855 | 0.225 |
| | | 0.1309 | 7.640 | 3.700 | 0.3052 | 0.0931 | 0.246 |
| | | 0.1451 | 6.989 | 0.397 | 0.0473 | 0.0022 | 0.006 |
| | | 0.1569 | 6.374 | 1.261 | 0.0253 | 0.0006 | 0.002 |
| | $f_1$ | 0.1722 | 5.809 | 1.366 | 5.9290 | 35.1530 | 92.707 |
| | | | | residual $SD^2$ | | 0.0124 | 0.033 |
| | | | | total power $Q$ | | 37.9192 | 100.000 |
| (H) 4.60 | | 0.0160 | 62.460 | * | * | * | * |
| | | 0.0342 | 29.240 | 12.841 | 0.0478 | 0.0023 | 0.004 |
| | | 0.0540 | 18.518 | 14.041 | 0.1331 | 0.0177 | 0.029 |
| | | 0.0667 | 14.995 | 1.276 | 0.1190 | 0.0142 | 0.024 |
| | $f_{1/2}$ | 0.0865 | 11.565 | 11.222 | 0.8427 | 0.7101 | 1.186 |
| | | 0.1060 | 9.436 | 8.424 | 0.1635 | 0.0267 | 0.045 |
| | | 0.1146 | 8.723 | 1.077 | 0.1358 | 0.0184 | 0.031 |
| | | 0.1193 | 8.382 | 2.350 | 0.4226 | 0.1786 | 0.298 |
| | | 0.1395 | 7.170 | 4.023 | 0.3801 | 0.1445 | 0.241 |
| | | 0.1527 | 6.551 | 5.761 | 0.1691 | 0.0286 | 0.048 |
| | $f_1$ | 0.1713 | 5.837 | 0.925 | 7.5628 | 57.1964 | 95.532 |
| | | | | residual $SD^2$ | | 0.0717 | 0.120 |
| | | | | total power $Q$ | | 59.8717 | 100.000 |
| (I) 5.7 | | 0.0490 | 20.420 | 9.313 | 0.2143 | 0.045922 | 0.088 |
| | | 0.0567 | 17.651 | 14.782 | 0.1075 | 0.011566 | 0.022 |
| | | 0.0600 | 16.665 | 16.366 | 0.5796 | 0.3359 | 0.646 |
| | | 0.0720 | 13.883 | 2.167 | 0.1007 | 0.0101 | 0.020 |
| | | 0.0875 | 11.434 | * | * | * | * |
| | | 0.0997 | 10.032 | 6.869 | 0.1922 | 0.0369 | 0.071 |
| | | 0.1107 | 9.036 | 6.030 | 1.4469 | 2.0935 | 4.023 |
| | | 0.1158 | 8.634 | 0.776 | 0.3227 | 0.1041 | 0.200 |
| | | 0.1224 | 8.169 | 2.617 | 0.8781 | 0.7721 | 1.482 |
| | | 0.1358 | 7.362 | * | * | * | * |
| | | 0.1475 | 6.778 | 0.946 | 0.3263 | 0.1065 | 0.205 |
| | | 0.1586 | 6.305 | 0.168 | 0.5703 | 0.3252 | 0.625 |
| | $f_1$ | 0.1711 | 5.846 | 1.653 | 6.5901 | 43.4294 | 83.459 |
| | | | | residual $SD^2$ | | 0.1448 | 0.278 |
| | | | | total power $Q$ | | 52.0363 | 99.801 |

J. Phys. Soc. Jpn. Downloaded from journals.jps.jp by University of California San Diego on 03/05/17



a complete bifurcation occurs. (The term "odd harmonics" is conventionally used in the present section. However, it will be discussed in the latter section §6 that this terminology is incorrect.)

Case (C) ($c = 4.1$): in additon to $f_1$ and $f_{1/2}$ and their harmonics previously observed, more spectral lines emerge from the positions of half frequency of $f_{1/2}$, that is, $f_{1/2}/2$ ($=f_{1/4}$) and its odd harmonics ($f_{3/4}$, $f_{5/4}$, $f_{7/4}$ and so on). The values of frequencies of these lines are also listed in Table II. We can see a complete bifurcation in this regime of parameter $c$.

A small spectral line is observed at the further half frequency $f_{1/4}/2$ ($=f_{1/8}$) and its odd subharmonics are also observed at due frequencies in Fig. 1. This may suggest that this parameter regime already undergoes the next subharmonic bifurcation though the contribution of these peaks to the total power is negligibly small.

*3.2.2 Inverse cascade*

Case (G) ($c = 4.30$): we can observe the subharmonics $f_{1/2}$ and $f_{1/4}$ as well as their odd harmonics in addition to the fundamental mode $f_1$ and its harmonics. However, no higher-order subharmonics $f_{1/8}$ and $f_{1/16}$ are observed. Many spectral lines are observed at frequencies close to higher-order subharmonic lines, but definitely shift from the position of higher-order subharmonic frequencies. For example, while spectral lines emerge from frequencies of 0.0562 and 0.0737, $f_{3/8}$-mode locates just at the middle of these two frequencies. No spectral line is observed at the position of this $f_{3/8}$-frequency.

Case (H) ($c = 4.60$): one subharmonic line $f_{1/2}$ and its odd harmonics can be recognized in addition to the fundamental mode $f_1$ and its harmonics. Like the case of $c = 4.30$, spectral lines close to higher-order subharmonics appreciably shift from due frequencies, and no spectral line can be observed at the subharmonic frequency $f_{1/4}$.

Thus, the processes of $c = 4.30$ and 4.60 should be understood to be the socalled "inverse cascade". The Lyapunov exponents calculated for these two parameters become positive, as seen in Fig. 3 in ref. 3 (or Fig. B.1 in ref. 1). These two states locate definite chaotic regime.

Case (I) ($c = 5.7$): more numerous discrete peaks are observed. It can be recognized that only the fundamental mode ($f_1$) and its harmonics emerge from normal frequency positions. $f_{1/2}$ subharmonic spectral line appears no longer at frequency of $f_{1/2}$.

The total number of spectral lines rather increase in the inverse cascade, as the growth of chaos. Higher-order subharmonics and their harmonics are considered to be modulated and buried with numerous emergences of spectral lines. The trend of MEM-PSD gradient in the inverse cascade is indicated by dashed line in Fig. 3.

*3.2.3 Transition region*

Case (D) ($c = 4.18$): as seen in Fig. 1(D), the pattern of spectral lines is extremely anomalous. We expected the next period-doubling of $f_{1/8}$ in this case, but we could observe no additional subharmonic higher-order peaks. We can see from the figure that $f_{1/4}$ subharmonic and its odd harmonic lines markedly broaden. We don't know whether this process indicates the onset of inverse cascade or not. This anomalous result may be related to the fact that the parameter $c = 4.18$ locates a critical region as seen in Fig. 3 in ref. 3 (or Fig. B.1 in ref. 1).

Case (E) ($c = 4.21$): further more spectral lines are observed. The frequencies of the lines exactly correspond to the subharmonics and its odd harmonics ($f_{1/8}$, $f_{1/4}$, $f_{3/8}$, $f_{5/8}$, $f_{3/4}$ and so on in the order from low frequency side) in addition to the fundamental mode ($f_1$) and its harmonics ($f_2$, $f_3$, $f_4$, and so on). Thus, the subharmonic bifurcations until $f_{1/8}$ can be ascertained in this case.

Case (F) ($c = 4.23$): Many spectral lines appears complicatedly. Surprisingly, all spectral lines observed exactly locate at the positions of frequency of spectral lines generated by the subharmonic bifurcations up to $f_{1/16}$. The frequency values of spectral lines are also listed in Table II. Parts of lines ($f_{1/16}$ and $f_{3/16}$) invisible and these are denoted by ( ) in the table.

From the above-mentioned results, we can ascertained that a cascade of complete subharmonic bifurcations occurs in the order of (A)→(B)→(C) and an inverse cascade (G)→(H)→(I). With respect to (D), (E) and (F) in the trasition region, (E) and (F) are considered to belong to the subharmonic cascade and (D) to the inverse cascade.

### *3.3 Contributions of subharmonics and harmonics to total power*

In order to investigate the contributions of subharmonics and harmonics to the total power, we calculated the least squares fitting (LSF) curve to the time series using a set of periodic modes corresponding to the fundamental mode, subharmonics and their harmonics (a part of which is listed in Table II).

*3.3.1 Evaluation procedure of contributions of powers*

The LSF curve is assumed to be expressed as

$$X(t) = A_0 + \sum_{n=1}^{N} A_n \cos\{2\pi f_n(t+\theta_n)\} + \varepsilon(t) \qquad (3)$$

where $f_n$ ($=1/T_n$) is the frequency of the $n$-th component ($T_n$: its period), $A_0$ a constant, $A_n$ and $\theta_n$ the amplitude and the phase of the $n$-th component, respectively, $N$ the total number of components, and $\varepsilon(t)$ the residual time series which are obtained by subtracting the LSF curve from the original time series.

The evaluation of LSF curve was performed by a procedure in ref. 16. The power of each periodic mode is evaluated by the square of amplitude, $A_i^2$, of $i$-th mode consitituting LSF curve. The relation between the contribution of each mode and the total power $Q$ is given by

$$\sum_{i=1}^{N} \frac{A_i^2}{Q} + \frac{r}{Q} = 1 \qquad (4)$$

where $r$ is the power of residual time series.

*3.3.2 LSF curves*

The optimum LSF curves to the original time series were calculated in the time range between 125 and 275 for each value of parameter $c$ and extended to the time ranges of 50–125 and 275–350. The residual time series were obtained by subtracting the optimum LSF curve from the original data. Figure 4 shows the residual

J. Phys. Soc. Jpn. Downloaded from journals.jps.jp by University of California San Diego on 03/05/17



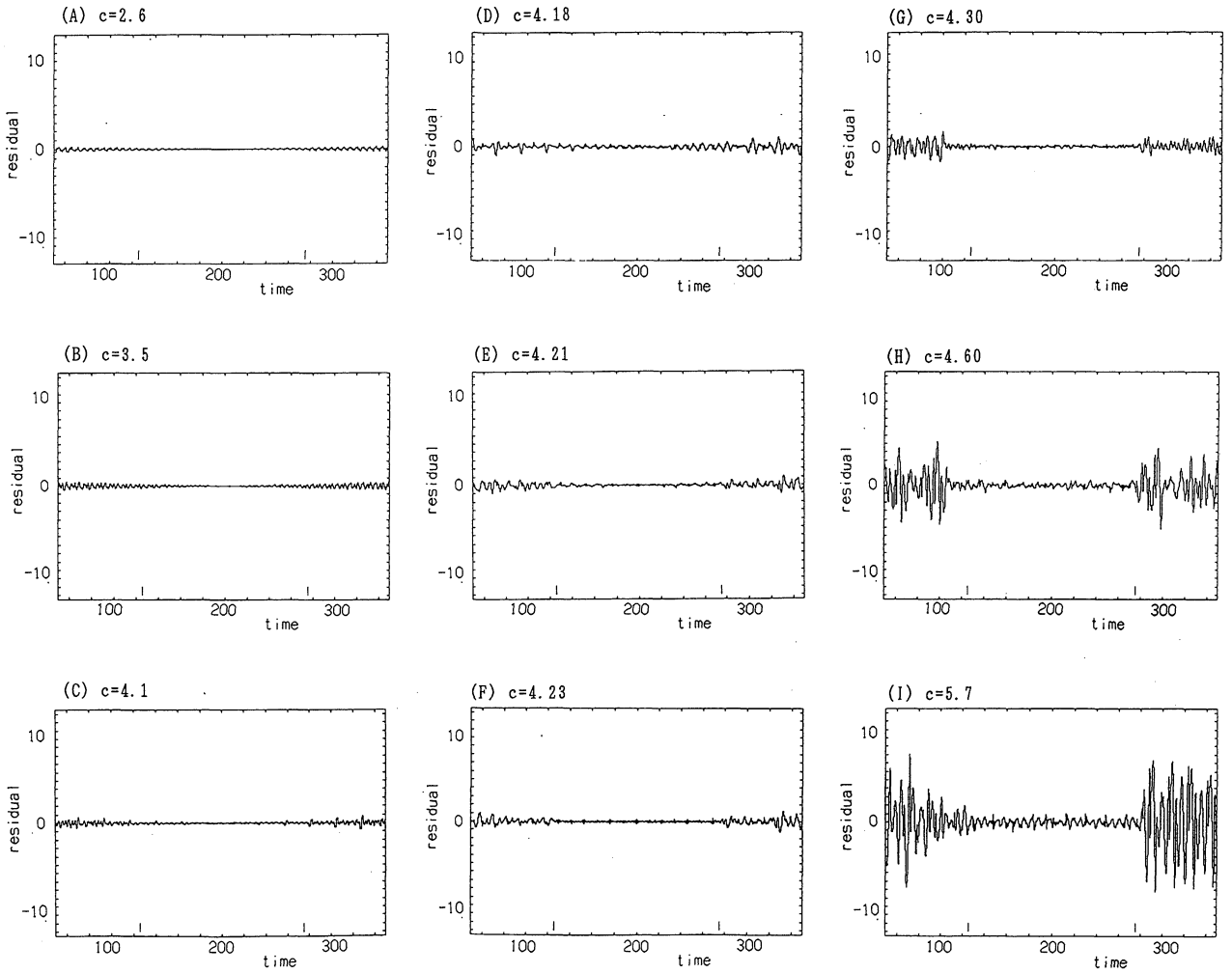


Fig. 4. Residual time series which is obtained by subtracting the original time series from the optimum LSF curve. Fitting (analysis) range and forward and backward prediction ranges. Two small vertical lines indicates the fitting range.

curves in the fitting range (125–275, denoted by two small vertical lines), including the residuals in the backward time range (50–125) and the forward time range (275–350). The results in backward and forward ranges will be used for prediction in §5.

The amplitudes of residual time series in the fitting range (125–275) are quite small. The optimum LSF curve thus obtained can satisfactorily reproduce the original time series. This suggests that every time series generated from Rossler model can be expressed by an appropriate superposition of several periodic functions. The time series for $c = 2.6$, 3.5, 4.1, 4.18 and 4.21–5.7 are reconstructed of 5, 11, 27, 30, 36 and 38 periodic functions, respectively. A part of the periods used for the fitting is listed in Table II, in which the periods up to $f_1$-mode are summarized. The amplitudes of residual time series in the fitting range slightly increase in the cases of $c = 4.60$ and 5.7. In the growth of chaos, 38 periodic modes are unsatisfactory for the LSF curve.

*3.3.3 Contributions of powers of spectral lines*

The contributions of powers of subharmonics and harmonics to the total power $A_i^2/Q$ are also listed in Table II for every parameter $c$. We can see from the table that the contirbution of the fundamental mode ($f_1$) is overwhelmingly large: it becomes larger than 90%. Namely, the time series of Rossler model can be said to be dominated by the fundamental mode. However, the LSF curve calculated with only one period ($1/f_1$) of fundamental mode never reproduce the original time series, because an accumulation of the contributions of other subharmonics and harmonics, which delicately shift their phases from each other, cannot be incorporated.

*3.3.4 Behaviors of fundamental mode*

We then examined in detail the behavior of fundamental mode (its frequency $f_1$). The variation of $f_1$ with the value of parameter $c$ is shown in Fig. 5(a) and the variation of the contribution to the total power $Q$ in Fig. 5(b). With increasing of $c$, $f_1$ gradually decreases from 0.1737 ($c = 2.6$) to 0.1711 ($c = 5.7$). The anomalous behaviors of $f_1$ are observed in the vicinity of $c = 4.2$ and this region corresponds to the transition region as pointed out in the preceding section. This is conjectured to relate with the anomalous spectral lines denoted in Fig. 1(D).

The contribution of $f_1$-mode to the total power gradually decreases as the value of $c$ increases: roughly seeing, from 99% at $c = 2.6$ to 83% at $c = 5.7$. Except for an anomalous change at the vicinity of $c = 4.21$, this trend corresponds to the fact that spectral lines increase

J. Phys. Soc. Jpn. Downloaded from journals.jps.jp by University of California San Diego on 03/05/17



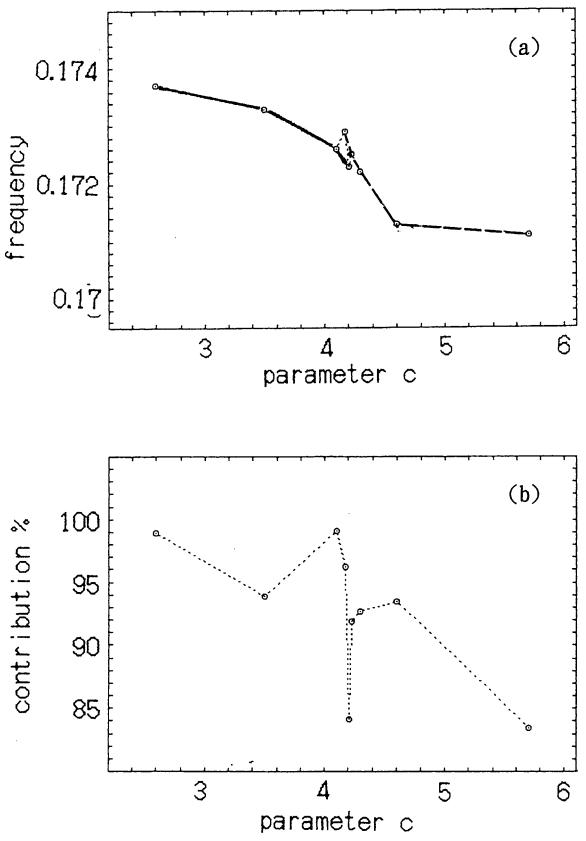


Fig. 5. Behavior of the fundamental mode. (a) the variation of the positions of frequency $f_1$, and (b) the contribution of $f_1$-mode to the total power.

in number as $c$ increases.

## §4. Segment Time Series Analysis

In order to investigate the temporal variation of PSD's, we divided the time series over 7200 points into many segments of 1000-point subseries beginning every 250 points and calculated PSD's for each segment. We then calculated the mean PSD by the procedure described in the preceding §3.1. 28 mean PSD's were thus obtained and the temporal variations of mean PSD's (linear scale) are displayed in Fig. 6 as the three-dimensional spectral array, taking frequency as the horizontal axis and time as its perpendicular axis from this side to the other side: the left side corresponding to the case of $c = 3.5$ and the right side the case of $c = 5.7$, for example.

$f_1$-peaks are marching in a fine array in the figure, although accompanied with large fluctuations of the amplitudes. Arrays of subharmonics and harmonics are negligibly small. This well-demonstrates the overwhelming contribution of $f_1$-mode stated in the preceding section.

The semi-log plots of the temporal variations of mean PSD's are demonstrated in Figs. 6(b) and 6(e). The gradient of log-PSD equals to the coefficient of exponent of exponential PSD's (eq. (2)), $-\lambda$. Figures 6(c) and 6(f) display the same PSD's taking time as the horizontal axis and frequency as its perpendicular axis. We can clearly see that all trends of PSD's are universally exponential, irrespective of the time range.

The magnitudes of $\lambda$ are listed in Table III except for the time range 0–50 considered to be a transient region. As seen from Figs. 6(b) and 6(c) and Table III, the $\lambda$'s in the case of $c = 3.5$ are almost constant irrespective of the variation of time, the variability of $\lambda$'s being within *ca* $\pm 0.026$ as the center at 3.949.

On the contrary, in the case of $c = 5.7$ (the growest state of chaos), the magnitudes of $\lambda$'s vary intermittently and the variability is within $-0.069$–$+0.127$ as the center at 2.693. This behavior is clearly seen in Figs. 6(e) and 6(f). This is considered to be one of marked characteristics of chaotic time series.

All values of $\lambda$'s listed in Table III are plotted in Fig. 7(a) and the average values of $\lambda$'s over the time range 125–275 (the analysis range) are connected by solid and dashed lines. A monotonous decreasing is shown in the figure. The average values of $\lambda$'s continuously decrease and the discontinuity in the vicinity of $c = 4.2$ shown in Fig. 3 is not ever observed. The difference between Fig. 3 and Fig. 7(a) may be caused by the difference of data length: the result in Fig. 3 was obtained for 3000-point data and that in Fig. 7(a) was the average value of $\lambda$ obtained for 1000-point data over the time range 125–275.

Figure 7(b) displays the variation of frequencies $f_1$ of the fundamental mode for 1000-point data averaged over the time range 125–275 (Table IV). The magnitudes of $f_1$ for $c = 4.18$–$4.2$ jut out remarkably from the overall trend. This is qualitatively consistent with the result in Fig. 5(a), although fluctuation of PSD for $c = 4.18$ becomes large.

## §5. Prediction

As seen in §3.3, the fittness of the optimum LSF curves to the original time series is quite preferable within the fitting range 125–275 indicated two small vertical lines as previously stated. Then, we extended the optimum LSF curves (eq. (3)) to two prediction ranges (backward time range 50–125 and forward time range 275–350). The fittness within the prediction ranges is also preferable in the cases of $c = 2.6$–$4.23$. Namely, the LSF curves well-reproduce the original time series.

On the other hand, in the cases of $c = 4.30$, 4.60 and 5.7, the amplitudes of residual time series within two prediction ranges gradually increase as the growth of chaos. This indicates a possibility of quantitative evaluation of the socalled "short-term" prediction of chaotic time series.

## §6. Discussion and Concluding Remarks

### *6.1 Fluctuations and route to chaos*

In the Rossler system, fluctuations caused by the nonlinearity already generate in the periodic stage of time series, and are stabilized (sturctured) in a series of cascade processes. The detailed implications will be described in the present section.

#### *6.1.1 $c = 2.6$: generation of fluctuations in the periodic time series*

The time series at $c = 2.6$ has been considered to be a fully periodic wave, that is, to exist in a stable state in which no subharmonics turn up. In fact, as seen in Fig. 1(A), the PSD for this periodic time series consists

J. Phys. Soc. Jpn. Downloaded from journals.jps.jp by University of California San Diego on 03/05/17



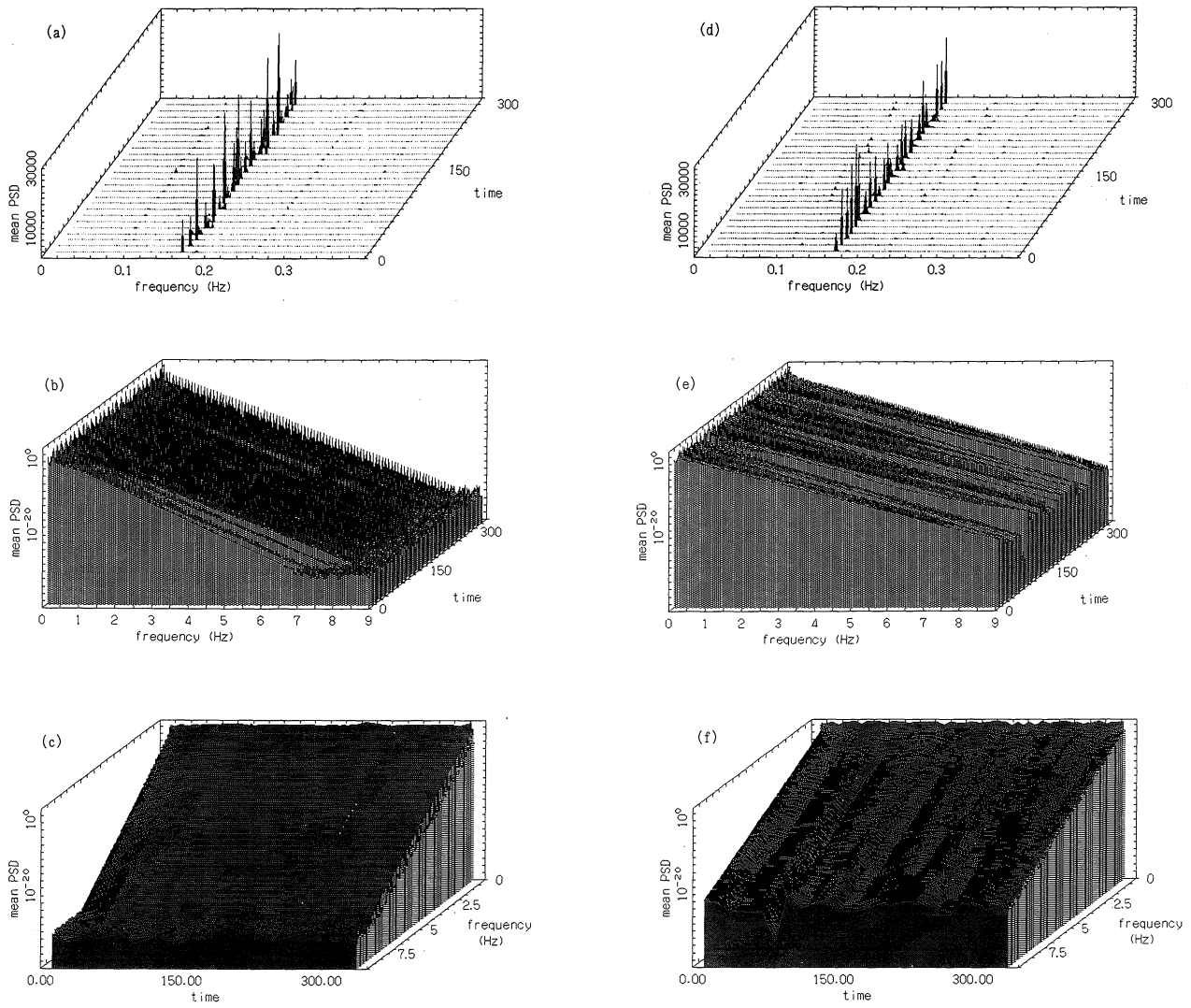


Fig. 6. 3 dimensional spectral array of the MEM-PSD. For the parameter $c = 3.5$, (a) linear scale, (b) and (c) semi-log scale, for the parameter $c = 5.7$, (d) linear scale, (e) and (f) semi-log scale.

Table III. Temporal variation of gradients of PSD's.

| $t$ \ $c$ | 2.6 | 3.5 | 4.1 | 4.18 | 4.21 | 4.23 | 4.30 | 4.60 | 5.7 |
|---|---|---|---|---|---|---|---|---|---|
| 125–175 | 5.487 | 3.922 | 3.466 | 3.566 | 3.407 | 3.416 | 3.494 | 3.242 | 2.632 |
| 150–200 | 5.607 | 3.961 | 3.474 | 3.557 | 3.408 | 3.376 | 3.367 | 3.233 | 2.820 |
| 175–225 | 5.569 | 3.946 | 3.463 | 3.543 | 3.395 | 3.387 | 3.345 | 3.214 | 2.725 |
| 200–250 | 5.638 | 3.944 | 3.461 | 3.464 | 3.401 | 3.437 | 3.344 | 3.231 | 2.643 |
| 225–275 | 5.668 | 3.974 | 3.460 | 3.412 | 3.520 | 3.396 | 3.363 | 3.160 | 2.646 |
| average | 5.594 | 3.949 | 3.465 | 3.508 | 3.426 | 3.402 | 3.383 | 3.216 | 2.693 |

of the fundamental mode $f_1$ and its harmonics $f_n = nf_1$ ($n = 2, 3, 4, \cdots$). However, exploring the time series shown in Fig. 1(A) in detail, an extremely small but systematical fluctuations can be recognized in the amplitudes of time series (see Fig. 8(a), the enlargement of the peak part of the time series). This fact is reflected in the phase trajectory drawn in Fig. 1(A). Figure 8(b) denotes the enlargement of the quite small rectangular region of the phase trajectory. Therein, we can see the anharmonicity of $c = 2.6$ trajectories.

As seen in Fig. 8(a), the amplitude of time series repeats alternately extensions and reductions with the period $2T_1$ on the average: $T_1$ is the fundamental period of the time series ($=1/f_1$). This behavior is drawn conceptionally in Fig. 8(c). From the consideration of a simple model, it is shown that this fluctuation results in the broad continuous peaks of PSD with the extermely small power generating at $f_n \pm f_{1/2}$ ($f_{1/2} = 1/(2T_1)$):

J. Phys. Soc. Jpn. Downloaded from journals.jps.jp by University of California San Diego on 03/05/17



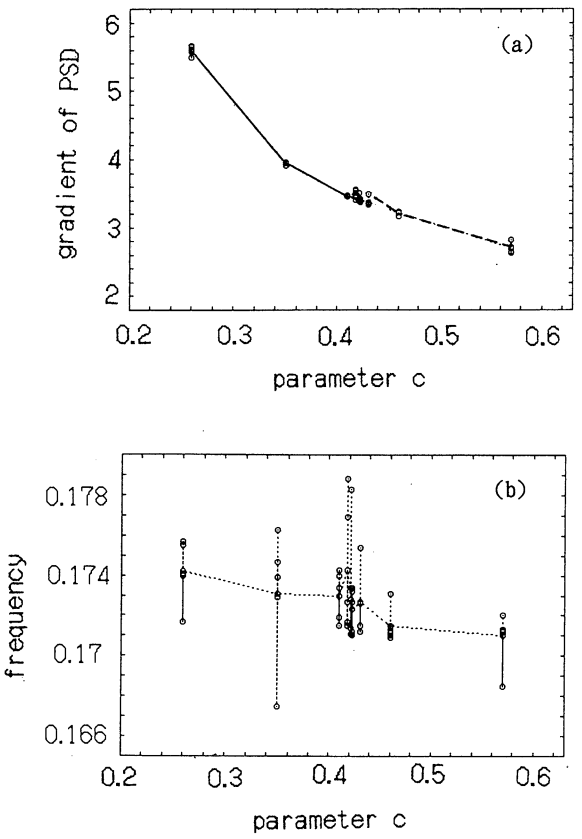


Fig. 7. Behavior of the fundamental mode based on segment time series. (a) the variation of the positions of frequency $f_1$, and (b) the contribution of $f_1$-mode to the total power.

the power being the order of $|a|^2|A_n|^2$, where $A_n$ is the amplitude of $f_n$ mode and $a$ the magnitude of amplitude fluctuation (the order of $10^{-4}$). In fact, these broad peaks are observed at the positions of $f_n \pm f_{1/2}$ in the PSD (Fig. 1(A)), and their powers exponentially decay in accordance to $|A_n|^2$ factor.

For simplicity, we consider a oscillator described as the form $x(t) = A\cos(ft - \phi)$, where $f$ is its frequency. Here, the amplitude $A$ is taken to fluctuate with the frequency $f'$ and the small amplitude $a$ around the average amplitude $\bar{A}$.

$$\begin{aligned} x(t) &= [1 + a\cos(f't - \phi')]\bar{A}\cos(ft - \phi) \\ &= \bar{A}\cos(ft - \phi) + 1/2a\bar{A}[\cos\{(f + f')t - (\phi + \phi')\} \\ &\quad + \cos\{(f - f')t - (\phi - \phi')\}] \end{aligned}$$

The PSD for $x(t)$ has spectral peaks at the positions of $f$ due to the first term and $f \pm f'$ due to the second term. The power of the latter spectral peaks becomes $\sim |a\bar{A}|^2$. Note that the model presented here is not the socalled "side band" model.

In the case of $c = 2.6$, $f = f_n$ $(n = 1, 2, 3, \cdots)$ and $f'$ fluctuates around $f_{1/2} = f_1/2$ on the average. Then, the PSD consists of the line spectral peaks at the positions of $f_n$ and the broad continuous peaks with the power of $|a\bar{A}_n|^2$ at $f_n \pm f_{1/2}$. In the case of $c = 3.5$, $f = nf_{1/2}$ and $f_n$ $(n = 1, 2, 3, \cdots)$ and $f' = f_{1/4}$, and so on.

*6.1.2 $c = 3.5$: subharmonic cascade and generation of new fluctuations*

In the case of $c = 3.5$, it can be seen in Fig. 1(B) that the PSD has spectral peaks at the exact positions of $f_n \pm f_{1/2}$. Namely, the broad continuous peaks caused by the amplitude fluctuations observed at $c = 2.6$ disappear and the periodic oscillations rise at the same positions of $f_n \pm f_{1/2}$ frequencies. This is considered to be that the fluctuation at $c = 2.6$ is stabilized at $c = 3.5$. At this moment, the new fluctuations of amplitudes generate with the period $2 \times 2T_1$ on the average, and the extremely small, broad peaks are observed at the positions of $nf_{1/2} \pm f_{1/4}$ $(f_{1/4} = 1/4T_1)$ in the PSD. Like the process from $c = 2.6$ to $c = 3.5$, these broad peaks stabilize as a periodic mode with $f_{1/4}$ at the next stage $c = 4.1$.

In the Rossler system, amplitude fluctuations are generated by an instability caused by the nonlinearity of the system and the frequencies of the fluctuations distribute around an average value, resulting in the continuous component of PSD. In the next stage, the fluctuations stabilize as a periodic oscillation of amplitudes with the average frequency only, that is, the broad continuum is structured.

*6.1.3 Inverse cascade process*

The inverse cascade can be regarded as a restructured process of the continuous region structured in the bifurcation cascade process, absorbing the subharmonic peaks and restructuring the regularity in part. For example, in the case of $c = 4.60$, the subharmonic spectral lines of $f_{1/8}$ and its harmonics are absorbed and disappear by the chaotic mixing, and then the spectral lines on both sides are affected. Namely, the region structured in the bifurcation process is restructured (the socalled continuous component of PSD in the chaotic mixing). Thus, in the inverse cascade, the whole continuous region grows as a "bundle" at $f_n \pm f_{1/2}$ with a more complicated structure, and the power of the bundle exponentially decays like the case of bifurcation cascade process.

Table IV. Frequency of fundamental mode $f_1$.

| $t$ \ $c$ | 2.6 | 3.5 | 4.1 | 4.18 | 4.21 | 4.23 | 4.30 | 4.60 | 5.7 |
|---|---|---|---|---|---|---|---|---|---|
| 125–175 | 0.1741 | 0.1747 | 0.1715 | 0.1717 | 0.1711 | 0.1712 | 0.1715 | 0.1710 | 0.1720 |
| 150–200 | 0.1755 | 0.1675 | 0.1740 | 0.1769 | 0.1783 | 0.1727 | 0.1754 | 0.1731 | 0.1685 |
| 175–225 | 0.1717 | 0.1739 | 0.1743 | 0.1788 | 0.1728 | 0.1732 | 0.1726 | 0.1709 | 0.1712 |
| 200–250 | 0.1740 | 0.1763 | 0.1719 | 0.1715 | 0.1714 | 0.1710 | 0.1712 | 0.1712 | 0.1720 |
| 225–275 | 0.1757 | 0.1729 | 0.1734 | 0.1727 | 0.1734 | 0.1734 | 0.1727 | 0.1714 | 0.1713 |
| average | 0.1742 | 0.1731 | 0.1730 | 0.1743 | 0.1734 | 0.1723 | 0.1727 | 0.1715 | 0.1710 |

J. Phys. Soc. Jpn. Downloaded from journals.jps.jp by University of California San Diego on 03/05/17



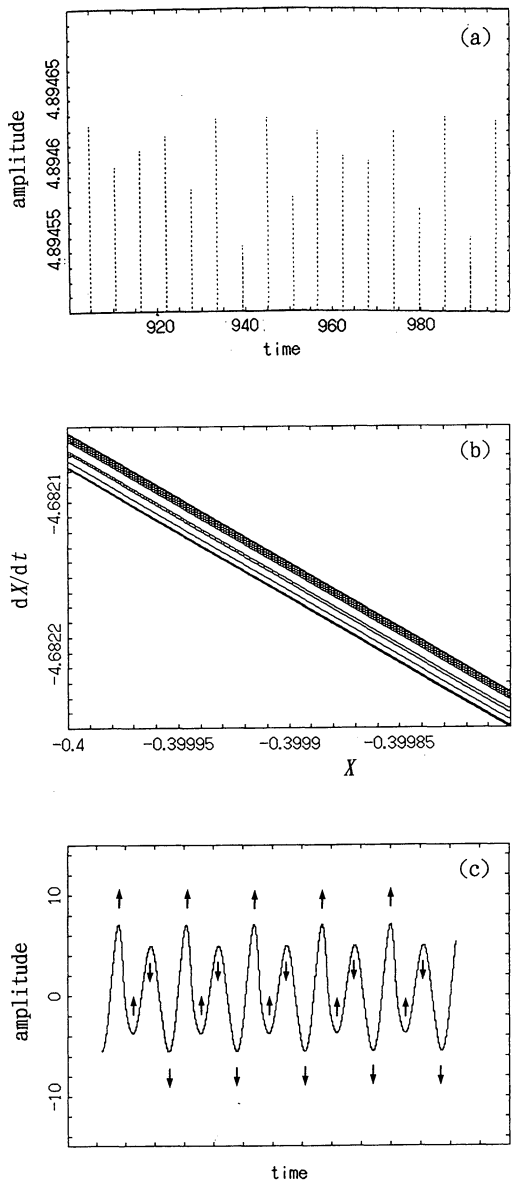


Fig. 8. Amplitude fluctuations of time series. (a) enlargement of the peak part of time series. (b) enlargement of the quite small rectangular region of the phase trajectory drawn in Fig. 1(A), and (c) conceptional interpretation of amplitude fluctuations of time series.

The remarkable feature of the above-mentioned picture is the following. First, the continuous component already generates in the parameter regions of periodic solutions and is structured as the periodic oscillations stabilized (the bifurcation cascade process). Next, the structured continuous region is newly restructured (the inverse cascade process).

### 6.2 *Exponential characteristics*

In our preceding work, we made an important finding that exponential characteristics of PSD were universally found for chaotic time series of Lorenz, Rossler and Duffing models. At that time, we considered that the exponential spectra may be related to nonlinear phenomena in general including the chaotic ones. Then, we investiagted in detail the PSD for Rossler model in the present study. As the result, we surely confirmed that the exponential characteristics are universally found for all time series generated by Rossler equation from the period bifurcations through the chaos, irrespective of variations of parameters and data lengths. Thus, it is conjectured that the exponential PSD is profoundly related to some nonlinearities. It is unknown what mechanism causes such exponential characteristics at present. The magnitudes of coefficients of the exponent ($\lambda$) depends on not only a type of nonlinear models but also the parameters used.

With respect to the exponential behavior of PSD, many experimental and theoretical studies have been reported so far.[4-12] Among them, we note two theoretical works on nonlinear Langevin equations: Frisch and Morf's[10] and Greenside *et al.*'s[11] ones. Frisch and Morf reported that the systems of nonlinearly coupled differential equations are expected to show exponentially decreasing power spectra at the higher frequencies. In their paper, Lorenz system and Burgers's model were also discussed to show the exponential PSD, and conjectures were moreover made about Navier-Stokes turbulence. Greenside *et al.* verified the exponetial dependence of PSD on frequency for the Lorenz model (see Fig. 11 in ref. 11), and stated that in the deterministic systems they did not observed a power law over any significant frequency range. A series of these theoretical studies as well as other experimental ones suggest our results. Thus, it is confirmed that the power spectrum of nonlinear systems including choas decreases exponentially in high frequency region.

In addition to the above descriptions, it is conjectured that the exponential characteristics of PSD in the dissipative systems such as Rossler and Lorenz models are the similar nature to the high frequency characteristics of the spectrum derived from a simple model of Hamiltonian system, that is, a universal nature for the system of nonlinear differential equations.[17] Therefore, this exponential characteristics give the following considerations on the time series. The time series must have frequency components until $f \to \infty$, without cut-off band of frequency. The power of spectrum $|A_n|^2$ has to exponentially decays beyond a higher mode of $N$ ($N$: integer), that is, at $n > N$.[17] As seen in the present results, $N$ is considered to be relatively small in Rossler system and $N = 2$–$3$ for $c = 2.6$ and 3.5.

### 6.3 *Contribution of the fundamental mode*

From the detailed spectral analysis in the present study, we obtained a surprising result that the contribution of the power of the fundamental mode to the total power is overwhelmingly large: it becomes larger than 90% as listed in Table II. This dominant character of the fundamental mode means that the system is essentially predominated by only one fundamental mode. That is, the fundamental mode is considered to play a key role in preservation of nonlinear phenomena.

Such dominant character of the fundamental mode and exponential characteristics of PSD's may be a basis for the socalled "structural stability." In our another report on a physiological data,[18] we also confirmed that the contribution of the fundamental mode becomes pre-

J. Phys. Soc. Jpn. Downloaded from journals.jps.jp by University of California San Diego on 03/05/17



dominantly large. This may be related to the socalled "homeostasis" in living bodies. The present study was the first to evaluate the the contribution of the fundamental mode, and that for Rossler model only. With respect to these speculations, further elucidations are required for any other nonlinear systems.

*6.4 Subharmonic cascade and inverse cascade*

Crutchfield *et al.* reported for Rossler model[3] that a cascade of subharmonic bifurcations occurs in relatively small values of parameter $c$ and thereafter an inverse cascade follows with increasing the parameter $c$. Moreover, Berge *et al.* stated in their textbook[1] that the inverse cascades accompanied by a gradual broadening of the lines of the Fourier spectrum, and hence the growth of chaos. With respect to these assertions, however, a slight amendment should be needed, taking consideration of the result revealed in the present study, as discussed in the preceding section (§6.1).

The present study gives the following results. Two regions corresponding to a cascade of subharmonic bifurcations and an inverse cascade are confirmed in the bifurcation process with increasing the parameter $c$, that is, in the former region, sequent subharmonic bifurcations appear and grow with increasing $c$, and, in the latter region, higher-order subharmonics and their harmonics are modulated and buried with numerous emergences of spectral lines with increasing the total number of spectral lines. There is a transition region between these two regions. We can conjecture that, in the transition region, subharmonics bifurcations are finally completed as structuring the continuous region and, simultaneously, the modulation of subharmonic bifurcations, that is, inverse cascade, occurs as restructuring the continuous region structured by the subharmonic cascade process.

*6.5 Predictability of chaotic time series*

Many works concerning time series prediction have been carried out so far and most recently some yields complied into a textbook (ref. 19). In that textbook, some marked methods for time series prediction, in particular, for chaotic time series prediction, are presented: autoregressive (AR) technique, state-space reconstruction by time-delay embedding and neural network etc. AR is unapplicable to chaos process because linear modeling based on AR process is considered to be impossible to describe nonlinear systems such as chaos. The other two methods are not easy to master the procedures of prediction.

The method proposed by the authors is fundamentally different from these methods. We use an extension of the optimum LSF curve of eq. (3) to the prediction ranges. There is a ground for this idea. As stated in ref. 14, our method is based on Wold's decomposition theorem[20] in which the PSD is described as a sum of two terms, predictable and unpredictable parts. Equation (3), except for $\varepsilon(t)$, exactly corresponds to the predictable part in Wold's decomposition theorem.

Our prediction procedure is quite useful for predicting time series with relatively high periodicity such as the case of sunspot number variations,[14] and also satisfactory for the case of chaos as well as all cases of subharmonic bifurcations in Rossler model as clarified in the present study. Thus, it can be said that our prediction method is also useful for the prediction of time series such as chaotic ones.

*6.6 Comment on the time range of time series used*

We must take some precautions for numerical calculations using nonlinearly coupled differential equations, becasue numerical solutions obtained are strongly dependent on the precision of data processing unit due to accumulation effect of errors caused by truncations and/or roundings. In order to examine this problem, we performed the calculations of time series to two kinds of significant digits for Rossler model: the one to 19 decimal places (the limit of significant digit for programming langauge C) and the other to 33 decimal places (multiple-precision of programming langauge UBASIC[21]). Moreover, the same calculations were carried out for Lorenz model for comparison.

In Fig. 9, the subtractions $(X_{19} - X_{33})$ of the time series to 19 decimal places $(X_{19})$ from those to 33 decimal places $(X_{33})$ for Rossler and Lorenz models are displayed. As seen in the figure, slight differences occur in the time range over 320 in the case of Rossler model. That is, time series $X_{19}$ substantially agrees with $X_{33}$ till the time 320. On the contrary, in the case of Lorenz model, remarked differences occur early near the time 70. Since we carried out the work on Lorenz model in the preceding study,[13] therein we used time series of 6000 points.

However, as seen in Table III in ref. 13, the values of

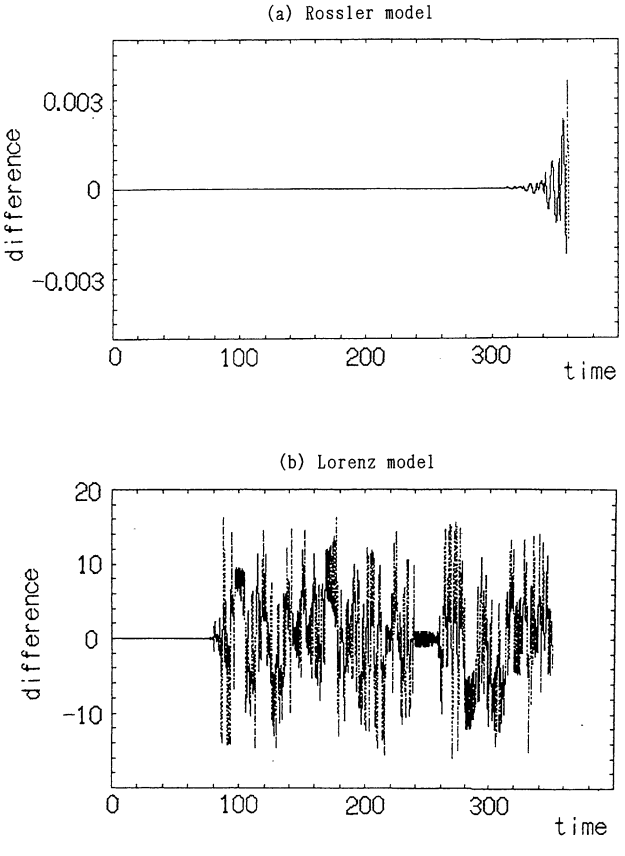


Fig. 9. Evaluation of the precision. (a) for Rossler model, and (b) for Lorenz model.

J. Phys. Soc. Jpn. Downloaded from journals.jps.jp by University of California San Diego on 03/05/17



$\lambda$ are strongly dependent on the wave form of segment time series in the case of Rossler model. This is caused by a transient behavior in this time range (<60). Except for this transient region and time range >320 (Fig. 9), we used the time series between 6000 and 32000 points corresponding to the time range 125–275 in the present study.

*6.7 Concluding remarks*

Theoretical elucidation of nonlinear systems will be expected to be attended with many unavoidable difficulties, though it remains to be an important subject from this time on. As a tentative measure, a superior and powerful tool for numerical calculations must be deviced for analysis of time series data. Especially, a developement of such tool is indispensable for comprehensively elucidating the complexity of chaotic system. The computing system for time series analysis, MemCalc, developed by the authors' group, is considered to be according to expectations. The computing system MemCalc based on Burg's algorithm in MEM enables us to calculate the PSD for any time series including chaotic ones with remarkably high accuracy. And using Wold's decompositon theorem we can reproduce the time series from the PSD estimated by MemCalc. Any modeling such as AR is not required for this computing process.

By the use of the MemCalc, a detailed study of power spectral densities was carried out for the time series numerically generated from the Rossler model from the period bifurcation process through the chaos. The following conclusions were obtained.

(1) All PSD's indicate an exponential decay with a large number of well-defined spectral lines until they level off at a limit determined by the accuracy of the present computation. The values of the coefficient of exponent, $\lambda$, become 5.582, 3.843, 3.124, 3.493, 3.124, 3.095, 3.388, 3.202 and 2.328 for the parameter $c = 2.6$, 3.5, 4.1, 4.18, 4.21, 4.23, 4.3, 4.6 and 5.7, respectively.

(2) The spectral lines observed are exactly corresponding to the fundamental mode, subharmonics, and their harmonics and a complete bifurcation up to the fifth-order period-doubling can be confirmed.

(3) From the results of investigations of values of $\lambda$ and the assignment of spectral lines, two regions corresponding to the subharmonic cascade and the inverse cascade are confirmed in the bifurcation process with increasing the parameter $c$. In the region of subharmonic cascade, sequent subharmonic bifurcations appear and grow and in the region of inverse cascade higher-order subharmonics and their harmonics are modulated and buried with numerous emergences of spectral lines with increasing the total number of spectral lines.

(4) The amplitude fluctuation of time series, resulting in the socalled broad continuum of PSD, caused by the nonlinearity of Rossler system, generates in the periodic stage and are stabilized (structured) in a series of cascade processes. The inverse cascade can be regarded as a restructured process of the continuous region structured in the bifurcation process.

(5) In the region of $c = 4.18$–4.21, an extremely anomalous behavior was recognized in the value of $\lambda$ and the pattern of spectral lines etc. This region is considered to be a transition region between two regions corresponding to the subharmonic cascade and the inverse cascade. In the transition region, it is conjectured that subharmonic bifurcations are finally completed and simultaneously the modulation of subharmonic bifurcations occurs.

(6) A surprising result was obtained that the contribution of the power of the fundamental mode to the total power is overwhelmingly large: it becomes larger than 90%.

(7) A time series prediction was performed by using an extension of the optimum least squares fitting curve and satisfactory results obtained indicated the usefulness of the present method for the prediction of time series including chaotic ones.


1) P. Berge, Y. Pomeau and C. Vidal: *Order within Chaos-Towards a Deterministic Approach to Turbulence* (John Wiley & Sons, New York, 1984).
2) H. Mori and Y. Kuramoto: *Sanitsu-Kouzou to Kaosu (Dissipation Structure and Chaos)* (Iwanami-Shoten, Tokyo, 1994) [in Japanese].
3) J. Crutchfield, D. Farmer, N. Packard, R. Shaw, G. Jones and R. J. Donnelly: Phys. Lett. **76A** (1980) 1.
4) A. Brandstater and H. L. Swinney: Phys. Rev. A **35** (1987) 2207.
5) X. Z. Wu, L. Kadanoff, A. Libchaber and M. Sano: Phys. Rev. Lett. **64** (1990) 2140.
6) K. Skold and K. E. Larson: Phys. Rev. **161** (1967) 102.
7) J. P. McTague, P. A. Fleury and D. B. DuPre: Phys. Rev. **188** (1969) 303.
8) B. J. Alder, J. C. Beer, H. L. Strauss and J. J. Weis: J. Chem. Phys. **70** (1979) 4091.
9) P. Atten, J. C. Lacroix and B. Malraison: Phys. Lett. **79A** (1980) 255.
10) U. Frisch and R. Morf: Phys. Rev. A **23** (1981) 2673.
11) H. S. Greenside, G. Ahlers, P. C. Hohenberg and R. W. Walden: Physica **5D** (1982) 322.
12) S. Kim, S. Ostlund and G. Yu: Physica D **31** (1988) 117.
13) N. Ohtomo, K. Tokiwano, Y. Tanaka, A. Sumi, S. Terachi and H. Konno: J. Phys. Soc. Jpn. **64** (1995) 1104.
14) N. Ohtomo, S. Terachi, Y. Tanaka, K. Tokiwano and N. Kaneko: Jpn. J. Appl. Phys. **33** (1994) 2821.
15) N. Ohtomo and Y. Tanaka: *A Recent Advance in Time-Series Analysis by Maximum Entropy Method* (Hokkaido University Press, Sapporo, 1994) p. 11.
16) S. Terachi, N. Ohtomo and Y. Tanaka: *A Recent Advance in Time-Series Analysis by Maximum Entropy Method* (Hokkaido University Press, Sapporo, 1994) p. 49.
17) G. M. Zaslavsky: *Chaos in Dynamic Systems* (Harwood Academic Publishers, London, 1985).
18) N. Ohtomo, Y. Tanaka, T. Kamo and K. Yoneyama: Jpn. J. Appl. Phys. **35** (1996) No. 10, in press.
19) *Time Series Prediction—Forecasting the Future and Understanding the Past—*, ed. A. S. Weigend and N. A. Gershenfeld (Addison-Wesley, New York, 1994).
20) A. Papoulis: *Probability, Random Variables, and Stochastic Processes* (MacGraw-Hill, New York, 1991) 3rd ed.
21) Y. Kida: UBASIC (Nippon-Hyouron-Sha, Tokyo, 1994) [in Japanese].